CELL CYCLE
2021, VOL. 20, NO. 13, 1242–1252
https://doi.org/10.1080/15384101.2021.1929677

Taylor & Francis
Taylor & Francis Group

RESEARCH PAPER

miR-665 inhibits epithelial-to-mesenchymal transition in bladder cancer via the SMAD3/SNAIL axis

Weiyu Wang, Yufan Ying, Haiyun Xie, Jiangfeng Li, Xueyou Ma, Liujia He, Mingjie Xu, Shiming Chen, Haixiang Shen, Xiangyi Zheng, Ben Liu, Xiao Wang, and Liping Xie

Department of Urology, First Affiliated Hospital, School of Medicine, Zhejiang University, Hangzhou, Zhejiang Province, China

ABSTRACT

Emerging research indicates that miRNAs can regulate cancer progression by influencing molecular pathways. Here, we studied miR-665, part of the DLK1-DIO3 miRNA cluster, which is downregulated by upstream methylation in bladder cancer. MiR-665 overexpression significantly downregulated the expression of SMAD3, phospho-SMAD3, and SNAIL, reversed epithelial–mesenchymal transition progression, and inhibited the migration of bladder cancer cells. To predict potential targets of miR-665, we used online databases and subsequently determined that miR-665 binds directly to the 3 untranslated region of SMAD3. Moreover, silencing of SMAD3 with small interfering RNAs phenocopied the effect of miR-665 overexpression, and overexpression of SMAD3 restored miR-665-overexpression-induced metastasis. This study revealed the role of the miR-665/SMAD3/SNAIL axis in bladder cancer, as well as the potential of miR-665 as a promising therapeutic target.

ARTICLE HISTORY
Received 21 June 2020
Revised 4 November 2020
Accepted 10 May 2021

KEYWORDS
miR-665; bladder cancer; migration; epithelial-mesenchymal transition

Introduction

Bladder cancer (BCa) is the tenth most common cancer worldwide. Annually, approximately 550,000 new cases are reported, and 200,000 people die due to BCa [1]. The cumulative risk of BCa to age 75 is higher in men than in women (1.08% and 0.27%, respectively) [2]. Europe has the highest prevalence of BCa, and the 5-year survival rate is only 68% [3]. Increased BCa incidence is attributable to a series of determinants including diabetes and nicotine use [4]. According to statistics, smoking is the major factor in BCa, and it triples the BCa risk relative to never smoking [5]. The BCa burden will inevitably increase, with an expanding elderly population [6]. At present, there is no effective way to treat BCa, which has a high recurrence rate even after surgical treatment [7]. Therefore, BCa pathogenesis requires further exploration to find new therapeutic targets.

MicroRNAs (miRNAs) are endogenous, noncoding RNAs that participate significantly in tumor pathology. Numerous studies recently confirmed that miRNAs could specifically identify the 3 untranslated region (3 -UTR) of targets, then induce the degradation of mRNA or prevent its translation [8]. Our research group has resolved many non-coding RNA and epigenetic relationships including miRNA, lncRNA, circRNA, and N6-methyladenosine modifications. In our previous work, miR-148a-3p, miR-124-3p, miR-323a-3p, miR-300, miR-433, miR-409, miR-101, miR-490-5p, and miR-26a were identified as having antitumor roles in BCa [9–17].

While exploring the mechanism of miRNAs, the DLK1-DIO3 genomic region attracted our attention. This large miRNA cluster encodes 54 miRNAs [18]. According to reports, most miRNAs in this cluster are abnormally expressed in tumors due to the regulation of upstream DNA methylation and are involved in various aspects of cellular homeostasis, like proliferation and metastasis [19,20]. Previously, we found that a series of miRNAs including miR-323a-3p, miR-300, and miR-433, all belonging to the DLK1-DIO3 miRNA cluster, were downregulated in BCa, and had a high methylation level in their upstream intergenic differentially methylated region (IG-

CONTACT Liping Xie xielp@zju.edu.cn
Supplemental data for this article can be accessed here

DMR) [11–13]. We wanted to identify other miRNAs within this imprinted domain also regulated by upstream DNA methylation.

In this study, we confirmed that miR-665, encoded by a part of the DLK1-DIO3 region, was downregulated by DNA methylation and reversed epithelial–mesenchymal transition (EMT) progression via regulation of the SMAD3 pathway. Our results provide a novel insight into the role of the miR-665/SMAD3/SNAIL axis in BCa.

Materials and methods

Cell lines and cell culture

We purchased T24 cells, UM-UC-3 cells, and a normal bladder epithelial cell line (SV-HUC -1) from the Chinese Academy of Sciences Cell Bank (Shanghai, China) and used short tandem repeat DNA analysis to confirm all of the above cell lines. We used RPMI 1640 medium to culture T24 and SV-HUC-1 cells and used MEM to culture UM-UC-3 cells. All cells were cultured with medium and 10% sterilized fetal bovine serum (FBS) at 37°C and 5% CO_2 in a humidified atmosphere.

Human clinical samples

From January 2011 to October 2013, paired BCa tissues and para-cancerous normal bladder mucosa tissues were obtained from patients undergoing radical cystectomy at the First Affiliated Hospital of Zhejiang University. The samples were collected after approval of the Ethics Committee, and informed consent was obtained. Samples were immediately preserved at −196°C. Clinical information is shown in Supplementary Table S1.

5-aza-CdR treatment

We treated T24 and UM-UC-3 cells with 5 μM 5-aza-CdR (Sigma, St Louis, MO, USA) for 4 days, then detected miR-665 expression at the RNA level.

Reagents and transfection

RNA duplexes were synthesized by GenePharma (Shanghai, China). The product sequences were as follows: hsa-miR-665 mimic (sense): 5-ACCAGGAGGCUGAGGCCCCU-3 and NC (sense): 5-UUCUCCGAACGUGUCACGUTT-3. The si-SMAD3 sequences were reported in a study on miR-323a-3p [11].

The effect of each siRNA sequence was verified. Three si-SMAD3 sequences were co-transfected in BCa cell lines to silence the target gene and avoid nonspecific effects. According to the manufacturer's protocol, the siRNA were transfected using Lipofectamine 2000 reagent (Invitrogen, Carlsbad, CA, USA). All plasmids were transfected with FuGENE HD Transfection Reagent (Promega, Madison, WI, USA).

RNA isolation and qRT-PCR

RNA was extracted with RNAiso plus (TaKaRa, Kusatsu, Japan) and then reverse transcribed with the One-Step PrimeScript miRNA cDNA Synthesis Kit and a PrimeScript RT reagent Kit. Using the ABI 7500 Fast Real-time PCR System, we detected RNA expression using SYBR Premix Ex Taq (TaKaRa, Kusatsu, Japan). GAPDH and small nuclear RNA U6 were used as endogenous references. The Livak method ($2^{-\Delta\Delta Ct}$) was used to calculate the data of associated gene expression. The primers used are shown in Supplementary Table S2.

Western blot analysis

We used RIPA lysis buffer to extract proteins, and the BCA Protein Assay kit to quantify the relative concentration. Proteins were loaded onto 10% SDS-polyacrylamide gels and subjected to electrophoresis. The wet transfer method was used to transfer the completely separated proteins to PVDF membranes. Fat-free milk was used to block the proteins for 1 h, then the membranes were incubated with the primary antibody (at 1:1000 dilution) at 4°C for 16 h. After washing with TBS-Tween buffer, the membranes were incubated with the secondary antibody (at 1:5000 dilution) at 25°C for 1 h. After the second wash

with TBS-Tween buffer, protein expression levels were detected using a chemiluminescence system (Pierce Biotechnology Inc., Rockford, IL, USA). All primary antibodies were as follows: rabbit anti-SMAD3, rabbit anti-SNAIL, rabbit anti-E-cadherin, rabbit anti-vimentin, and rabbit anti-GAPDH (Proteintech Group Inc., Rosemont, USA), and anti-p-SMAD3 (Ser423/425) (Cell Signaling Technology, Beverly, MA, USA).

Dual-luciferase reporter assay

Oligonucleotide pairs were purchased from Sangon (Shanghai, China). Segments containing the miR-665 target or mutant region were inserted into the pmirGLO Dual-Luciferase miRNA Target Expression Vector (Promega) between SacI and SalI sites. DNA sequencing was used to verify the insertions. In 24-well plates, T24 cells were co-transfected with 100 ng of reporter pmirGLO and 50 nM miR-665 or NC. Relative activity of luciferase was detected after 48 h using the Dual-Luciferase Reporter Assay System (Promega).

Wound healing assay

A cross wound was made in the transfected cell monolayer once T24 cells cultured in six-well plates reached 100% confluence. Cells were cultured in serum-free medium for one day, and wound healing was observed using phase-contrast microscopy (Olympus, Tokyo, Japan).

Transwell assay

Cell migration was evaluated using the Boyden chamber, or transwell assay (Millipore, Boston, MA, USA). Transfected T24 or UM-UC-3 cells (6×10^4) were suspended in 300 µl medium (FBS-free) and placed onto the surface layer of the chambers. The chambers were placed in a 24-well plate and 600 µL medium (with 10% FBS) added to the outer compartment. Cells were fixed with methanol and stained using 0.1% crystal violet after one day incubation at 37°C. Cells on the membrane (upper surface) were carefully cleaned with a cotton swab. Phase-contrast microscopy (CARL ZEISS, Germany) was used for imaging with a 10× objective.

Statistical analysis

We expressed data as the mean ± standard deviation (S.D.) and adopted Student's t-test to estimate the differences. The data were analyzed using SPSS 22 software (IBM, Armonk, NY, USA). Significance was defined as a two-tailed p-value of <0.05.

Results

Low expression of miR-665 in BCa

We detected the expression of miR-665 in BCa cell lines. miR-665 expression was significantly down-regulated in T24 and UM-UC-3 cells compared to that in immortalized normal bladder epithelial cells (SV-HUC-1) (Figure 1 (a)). miR-665 levels in BCa and para-cancerous tissues of eight patients was reduced relative to those in normal tissues (Figure 1 (b)). As low miRNA expression usually indicates an antitumor function, we used an online database (https://kmplot.com/analysis) to perform Kaplan-Meier survival analysis of BCa relative to miR-665 expression and found that high miR-665 expression was significantly associated with a high overall survival rate ($P = 0.022$, Figure 1 (c)). Based on the above analysis, we predict miR-665 to be a tumor suppressor in BCa.

Next, we explored the link between miR-665 expression and DNA methylation. 5-aza-2-deoxycytidine (5-aza-CdR) inhibits DNA methyltransferase, an enzyme that regulates transcription of downstream regions by altering upstream DNA methylation levels. As expected, miR-665 expression in T24 and UM-UC-3 cells increased significantly after 5-aza-CdR treatment (Figure 1 (d)). These results suggest that DNA methylation may play a significant role in decreased expression of miR-665.

Overexpression of miR-665 suppresses the migration of BCa cells by inhibiting EMT

We conducted gain-of-function experiments to investigate the role of miR-665. Wound healing and transwell assays consistently showed that miR-665 could inhibit migration in T24 and UM-UC-3 cells (Figure 2 (a-c)). According to emerging studies, EMT is closely related to tumor metastasis [21,22];

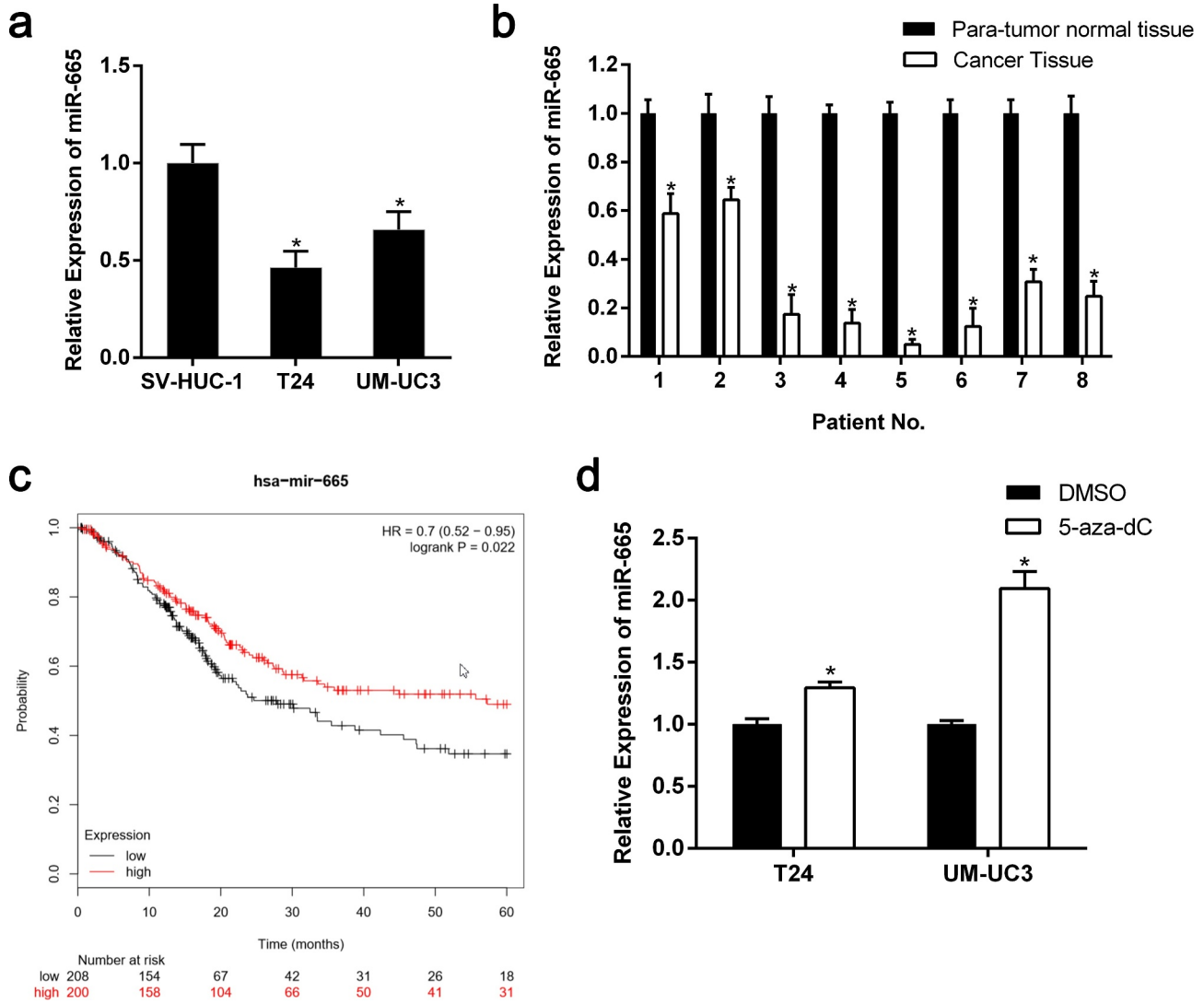

Figure 1. Downregulation of miR-665 in BCa. (a) miR-665 expressions in T24 and UM-UC3 cell lines were significantly downregulated compared to that in the normal bladder cell line (SV-HUC-1). (b) Relative expression of miR-665 in BCa and para-cancerous tissues of eight patients were confirmed by qRT-PCR. (c) Kaplan-Meier survival analysis indicated that high miR-665 expression was significantly associated with a high overall survival rate of BCa. (d) miR-665 expression was significantly increased in T24 and UM-UC3 cell lines after treatment with a demethylation agent. Error bars represent the S.D. obtained from three independent experiments; *P < 0.05.

therefore, we investigated the changes in EMT biomarkers. Western blot assays showed that the expression of E-cadherin was significantly upregulated in T24 and UM-UC-3 cells after miR-665 transfection, while the protein levels of vimentin and SNAIL were significantly downregulated (Figure 2 (d)). These results suggest that miR-665 overexpression significantly reverses EMT progression in BCa.

miR-665 downregulates SMAD3 by binding its 3 -UTR

To identify possible targets of miR-665, we searched online databases (TargetScan, http://www.targetscan.org and starbase2.0, http://starbase.sysu.edu.cn/starbase2). Based on bioinformatics prediction results, we selected six target genes and found that the mRNA of SMAD3 was

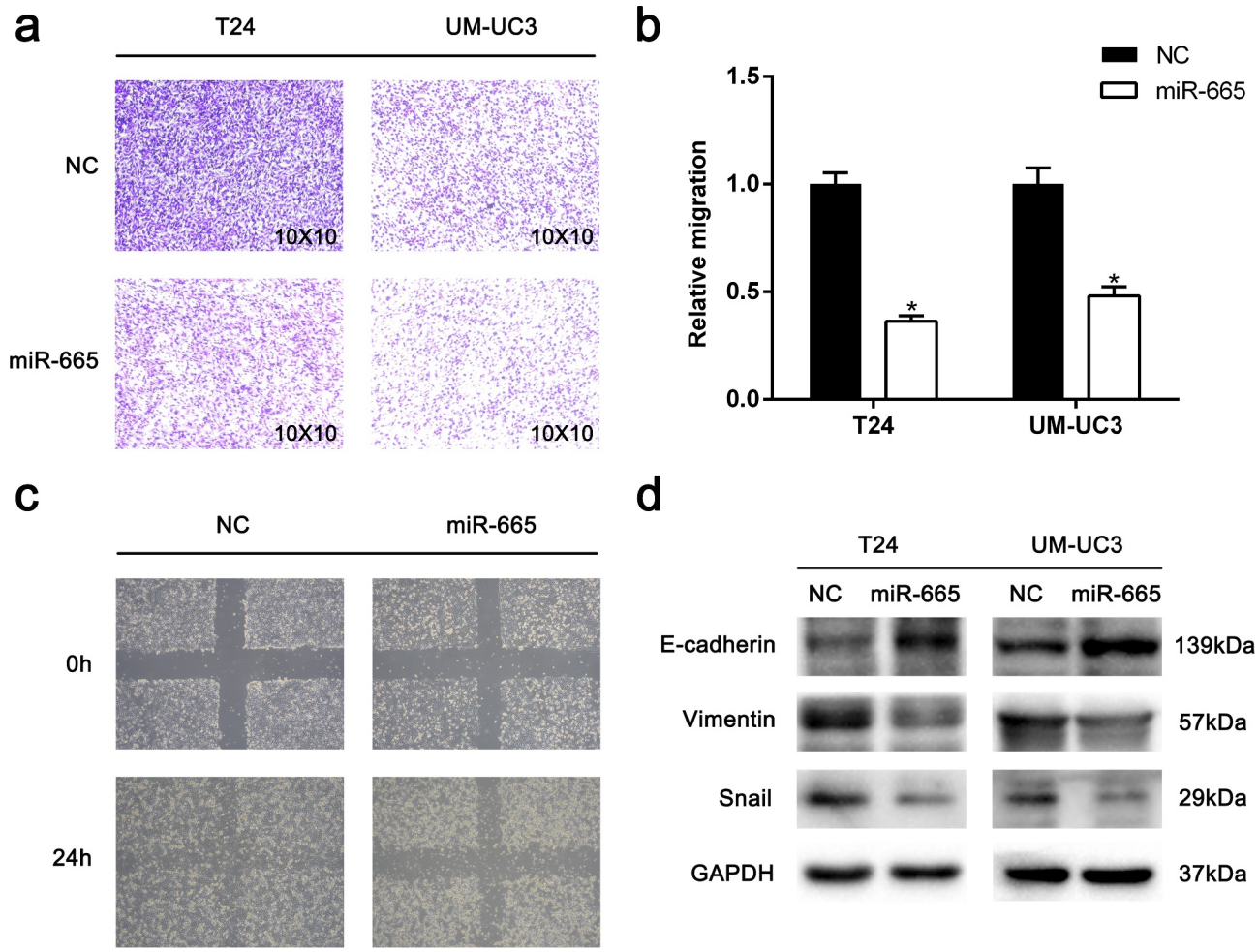

Figure 2. miR-665 significantly inhibits the migration and EMT of BCa cells. T24 cells and UM-UC3 cells were transfected with miR-665 mimics (50 nM). (a) Transwell assays showed that the migration of T24 and UM-UC3 cells was inhibited after transfection. Images of the transwell assay were obtained under an 10× objective. (b) The representative micrograph of the transwell assay was calculated. (c) A wound healing assay showed that miR-665 significantly inhibited the migration of T24 cells. (d) Western blotting showed that miR-665 changed concentrations of EMT-related proteins in T24 and UM-UC3 cell lines. Error bars represent the S. D. obtained from three independent experiments; *P < 0.05.

significantly downregulated in T24 cells after transfection with miR-665 mimics (Figure 3 (a)). Verification in the UM-UC-3 cell line showed similar results (Figure 3 (b)). EMT of multiple tumors involves phosphorylation of SMAD3 [23–25].

Western blot assays revealed that SMAD3 and phospho-SMAD3 (p-SMAD3) were significantly downregulated in T24 and UM-UC-3 cells after treatment with miR-665 mimics (Figure 3 (c)). Based on these results, we speculated that SMAD3 is the target of miR-665. Luciferase reporter assays showed that SMAD3 wild-type luciferase activity was significantly reduced in T24 cells after miR-665 treatment, while the mutant group activity showed no significant change (Figure 3 (d)). Wild-type binding site and mutation site sequences of miR-665 are shown in Figure 3 (e).

Knockdown of SMAD3 suppresses migration and EMT

We speculated that miR-665 suppresses migration and EMT progression in BCa by binding SMAD3. By searching the Oncomine online database (www.oncomine.org), we found that SMAD3 expression in superficial BCa was significantly higher than that in normal bladder mucosa (Figure 4 (a), P = 0.016, significant). To further

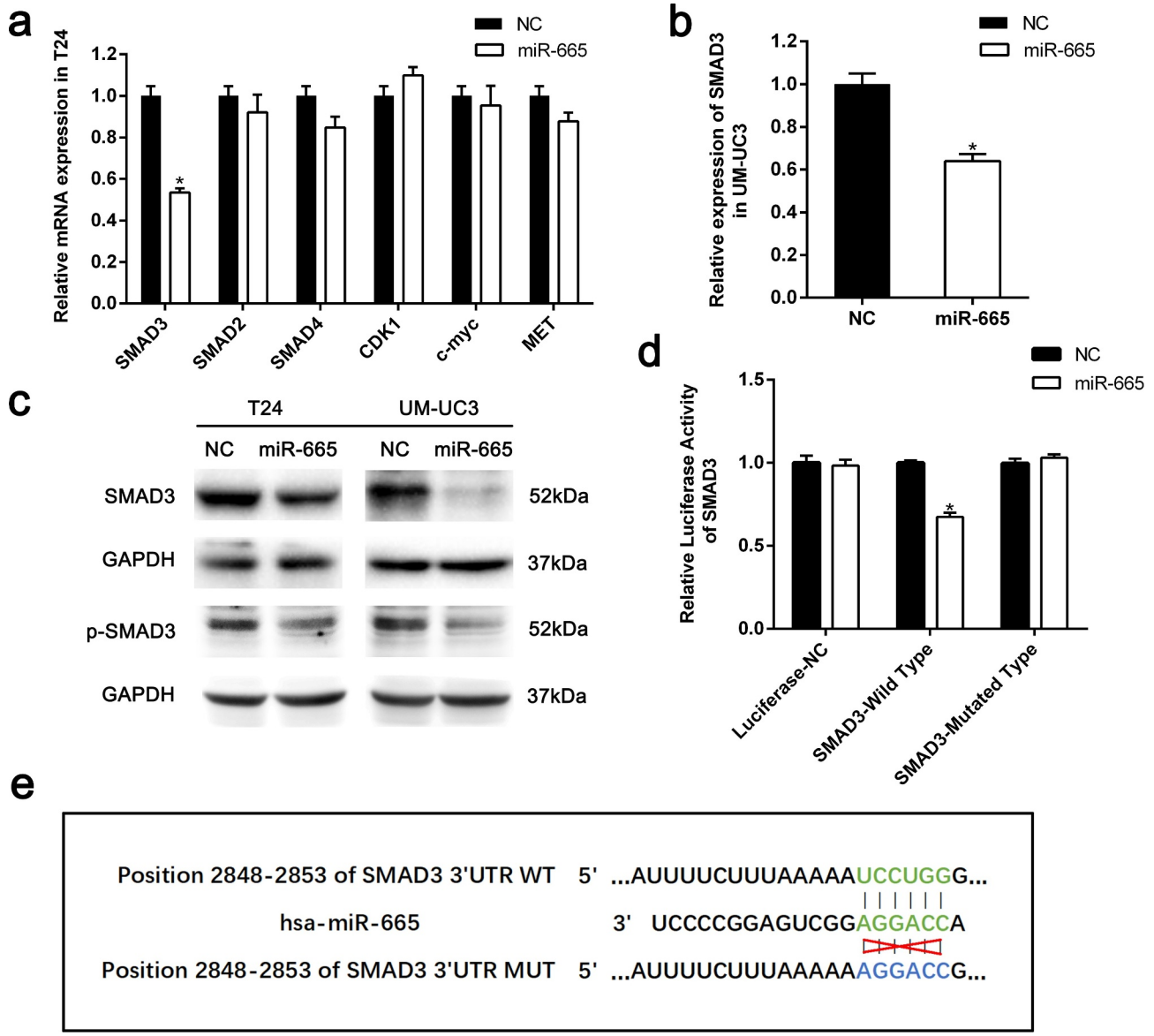

Figure 3. miR-665 targets SMAD3 in BCa. (a-b) qRT-PCR experiments showed that SMAD3 was significantly downregulated at the RNA level in T24 and UM-UC3 cell lines after transfection with miR-665 mimics. (c) Western blot assays showed significant SMAD3 downregulation at the protein level in T24 and UM-UC3 cells after transfection with miR-665 mimics. (d) Dual-luciferase reporter assay demonstrated that miR-665 significantly inhibited the luciferase activity of vectors that carried the 3 -UTR of SMAD3 in T24 cells. (e) miR-665 target sites in the 3 -UTR of SMAD3 were mutated as represented. Error bars represent the S.D. obtained from three independent experiments; *P < 0.05.

verify the effect of SMAD3, we used small interfering RNA (siRNA) to silence SMAD3. To avoid nonspecific effects, we used different siRNA sequences for cotransfection and verified the knockdown efficiency of each siRNA (Figure 4 (b)). Wound healing and transwell assays indicated that the migration of T24 and UM-UC-3 cells was significantly inhibited after si-SMAD3 treatment (Figure 4 (c-e)). Western blot assays showed that E-cadherin expression in T24 and UM-UC-3 cells was upregulated after treatment with si-SMAD3, while the expressions of p-SMAD3, SNAIL, and vimentin were downregulated (Figure 4 (f)). The effect of silencing SMAD3 is consistent with that of miR-665 overexpression in BCa.

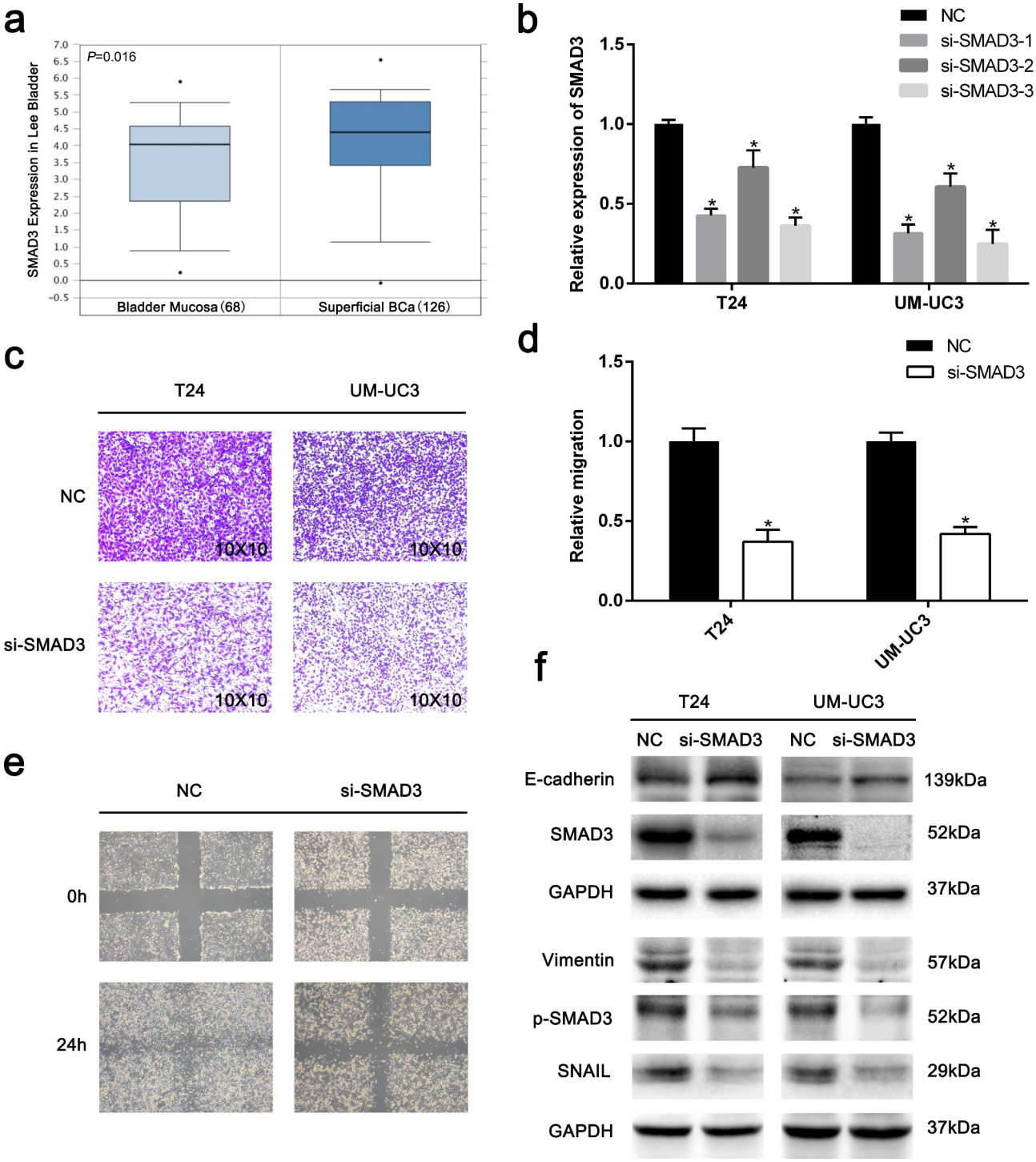

Figure 4. Knockdown of SMAD3 using siRNAs shows significant inhibition of EMT and migration in BCa. (a) The Oncomine online database showed that the expression level of SMAD3 in BCa was significantly higher than that in normal bladder mucosa (P = 0.016, significant). (b) The knockdown efficiency of each siRNA was verified by using qRT-PCR. (c) In transwell assays, migration of T24 and UM-UC3 cells was inhibited after treatment with si-SMAD3. The images were obtained and analyzed under a 10x objective. (d) The representative micrograph of the transwell assay was calculated. (e) A wound healing assay showed that treatment with si-SMAD3 significantly inhibited the migration of T24 cells. (f) Western blot assay confirmed that treatment with si-SMAD3 inhibited EMT. Error bars represent the S.D. obtained from three independent experiments; *P < 0.05.

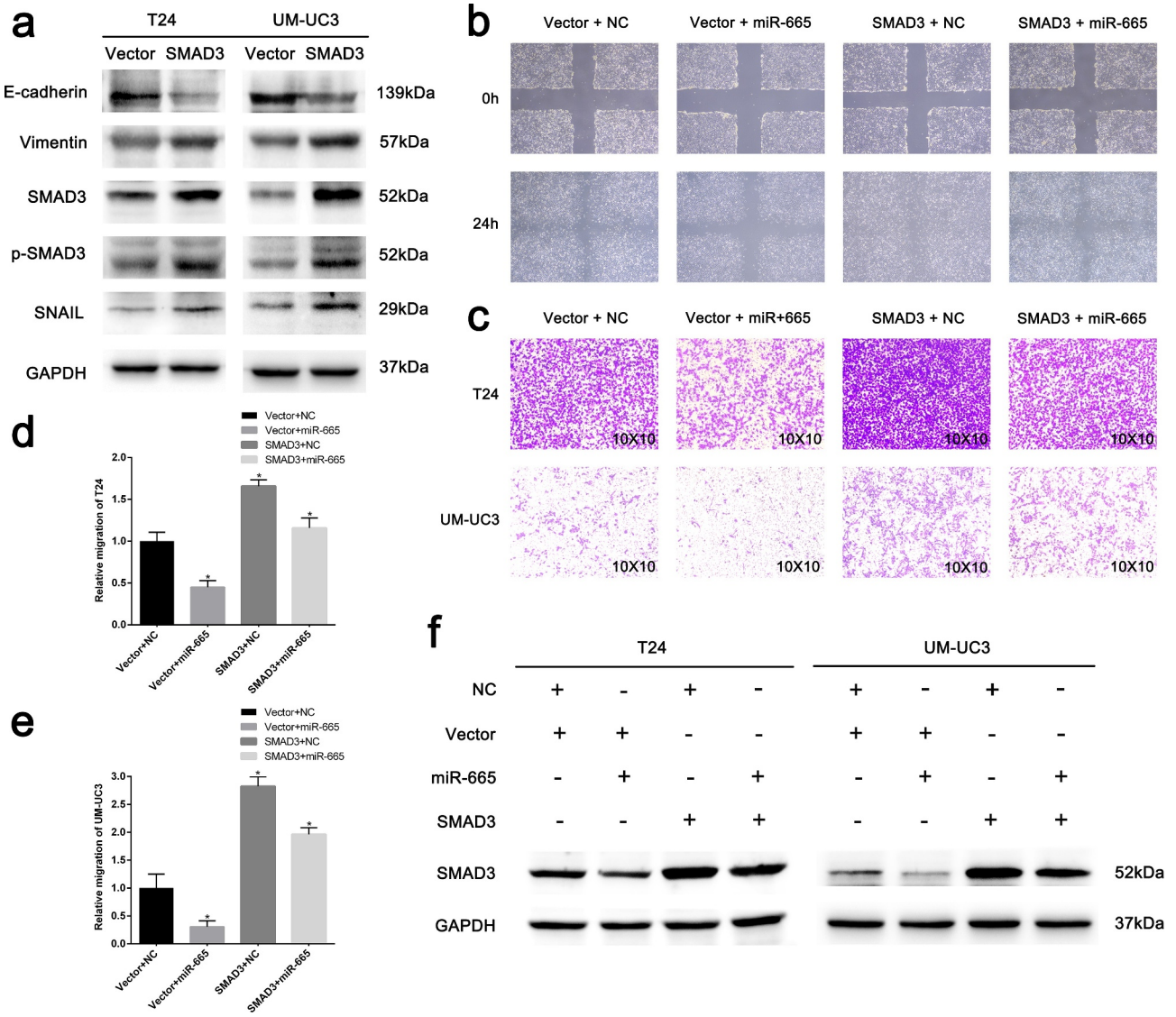

Figure 5. SMAD3 overexpression rescues miR-665-overexpression-induced suppression of EMT in BCa. (a) The changes of EMT markers at protein levels after treatment with SMAD3-overexpressing plasmids. (b) A wound healing assay showed that the co-transfection of miR-665 and SMAD3 plasmid reversed migratory inhibition induced by miR-665 overexpression in T24 cells. (c) Transwell assays consistently indicated that the co-transfection of miR-665 and SMAD3 plasmid reversed migratory inhibition induced by miR-665 overexpression in T24 and UM-UC3 cells. Images were obtained and analyzed under a 10x objective. (d-e) The relative migration rates of T24 and UM-UC3 cells were calculated. (f) Western blot assay confirmed SMAD3 protein expression levels were consistent with the phenotype in T24 and UM-UC3 cells. Error bars represent the S.D. obtained from three independent experiments; *P < 0.05.

SMAD3 overexpression rescues miR-665-overexpression-induced suppression of EMT in BCa

The changes of EMT markers at protein levels suggested that overexpression of SMAD3 could promote EMT in T24 and UM-UC-3 cells. (Figure 5 (a)). To further evaluate the binding relationship between miR-665 and SMAD3, we used miR-665 and SMAD3-overexpressing plasmids to conduct rescue experiments. Wound healing and Transwell assays showed that the migration of T24 and UM-UC-3 cells was enhanced by the overexpression of SMAD3. More importantly, miR-665-overexpression -induced migration inhibition was significantly reversed by co-transfection with the SMAD3 plasmid (Figure 5 (b-e)). As expected, changes in SMAD3 at the protein level were consistent with the phenotype in T24 and UM-UC-3 cells (Figure 5 (f)). A second rescue experiment with miR-665 inhibitor and si-

SMAD3 was conducted using another approach and the results again supported SMAD3 as a target of miR-665. Changes in protein levels in gain-of-function experiments suggested that knockdown of SMAD3 could inhibit progression of EMT induced by miR-665 downregulation in T24 and UM-UC3 cell lines (Supplementary Figure 1 (a-e)). Based on these findings, SMAD3 downregulation may explain why miR-665 can inhibit the migration of BCa cells. Our results indicate that miR-665, as a regulatory factor of SMAD3, plays a tumor suppressor role in the metastasis and pathogenesis of BCa.

Discussion

Emerging evidence has confirmed that miRNAs are instrumental in cancer pathogenesis. They can specifically bind to the 3 -UTR of mRNAs regulating their degradation and inhibiting their translation [8]. MiR-665, part of the DLK1-DIO3 miRNA cluster, is located in the 14q32.2 chromosomal region. miR-665 functions as a tumor suppressor in pancreatic cancer, gastric cancer, retinoblastoma, and other types of tumors [18,26–28]. However, the function of miR-665 in BCa remains unknown. In this study, we demonstrated that miR-665 suppresses EMT and migration by targeting SMAD3 in BCa cells.

Previous studies have shown transcriptional regulation of downstream genes relies on upstream DNA methylation. Many tumor suppressor genes are usually silenced due to the methylation of their upstream regions [29]. The DLK1-DIO3 miRNA cluster, which encodes many antitumor miRNAs, is located on human chromosome 14q32. Emerging studies have confirmed that these miRNAs are usually silenced by methylation of the upstream intergenic differentially methylated region (IG-DMR) [19,20]. Our previous work showed that numerous DLK1-DIO3 cluster miRNAs like miR-323a-3p and miR-433, were also downregulated in BCa, and exhibited a high methylation level in the IG-DMR region [11–13]. MiR-665 neighbors the miRNAs mentioned above. As expected, qRT-PCR results showed miR-665 significantly upregulated expression after methyltransferase (5-aza-CdR) treatment. These results support our hypothesis that upstream IG-DMR methylation of the DLK1-DIO3 domain can downregulate miR-665.

EMT refers to the process by which normal epithelial cells gradually lose their epithelial phenotype and transform into a mesenchymal phenotype whereby gaining new characteristics such as invasion, migration, and antiapoptosis [30]. Signaling pathways, including epidermal growth factor (EGF) and transforming growth factor-β (TGF-β) regulate EMT [22,31–33]. Non-coding RNA also transforms EMT. Expression of related biomarkers changes once EMT occurs; for instance, SNAIL and E-cadherin changes are negatively correlated. Migration of BCa cells was inhibited in our gain-of-function experiments after inducing miR-665-overexpression. Western blot assays demonstrated consistent relative changes in EMT biomarkers. For instance, E-cadherin expression was upregulated, while SNAIL and vimentin expression was downregulated. This evidence supports that miR-665 can suppress migration and EMT in BCa cells.

SMAD3 and SNAIL are strongly associated key proteins involved in EMT progression. A study of 103 patients showed high SMAD3 expression in urothelial tumors indicates poor overall survival [34]. SMAD3, as a substrate of TGF-β receptor kinase, is an important transcription factor. SMAD3 is activated by phosphorylation, and transmits signals to the cell nucleus and initiates the transcription of SNAIL [23,24,35]. SNAIL, another major component of EMT, not only induces the expression of ZEB1, MMP2, MMP9, and other migration-related proteins, but also recruits polycomb repressive complex 2 (PRC2) to directly bind to the promoter of E-cadherin inhibiting transcription [36–38]. Interestingly, SNAIL and SMAD3/4 promote EMT by forming a transcriptional repressor complex of E-cadherin, occludin, claudin-3, and CAR [39,40]. In this study, the expression of SMAD3, p-SMAD3, and SNAIL was downregulated after induced miR-665-overexpression, and dual-luciferase reporter assays confirmed that miR-665 directly targeted the 3 -UTR of SMAD3. Furthermore, siRNA knockdown of SMAD3 in T24 and UM-UC-3 cells showed that SNAIL expression and EMT progression were both inhibited, consistent with our previous research on miR-323a-3p [11]. Additionally, rescue experiments to investigate the antagonistic effect of miR-665-overexpression and SMAD3-overexpression, supported our view that miR-665 can suppress SNAIL expression and BCa migration by targeting SMAD3.

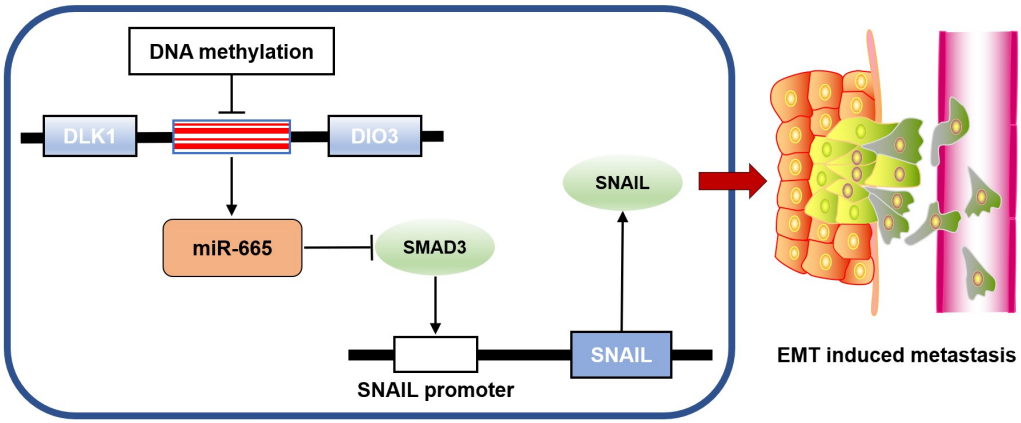

Figure 6. miR-665 mediates the SMAD3/SNAIL pathway in BCa. This schematic diagram represents the inhibited migration of BCa cells via the miR-665/SMAD3/SNAIL pathway and the dysregulation of miR-665 due to upstream DNA methylation.

Our study supports that miR-665 is downregulated by methylation of upstream DNA. By targeting SMAD3, miR-665 downregulates SNAIL expression, reverses EMT progression, thus inhibiting the migration of BCa cells. Therefore, the miR-665/SMAD3/SNAIL axis demonstrated regulation of BCa cell migration (Figure 6 (a)). The miR-665 mechanism revealed by this study may offer a novel approach to the specific treatment of BCa.

Acknowledgments

This work was supported by grants from the National Natural Science Foundation of China (grant no.81772744, 81802564, 81874203, 81902612 and 81972374), the Zhejiang Provincial Natural Science Foundation of China (LY20H160030, LY20H160022), the Zhejiang Province Medical and Health Scientific Research Project (2019RC033) and the China Postdoctoral Science Foundation (2018M632489).

Disclosure statement

No potential conflict of interest was reported by the author(s).

Funding

This work was supported by the China Postdoctoral Science Foundation [2018M632489]; National Natural Science Foundation of China [81802564]; National Natural Science Foundation of China [81874203]; National Natural Science Foundation of China [81902612]; National Natural Science Foundation of China [81772744]; National Natural Science Foundation of China [81972374]; Zhejiang Provincial Natural Science Foundation of China [LY20H160022]; Zhejiang Province Medical and Health Scientific Research Project [2019RC033]; Zhejiang Provincial Natural Science Foundation of China [LY20H160030].

ORCID

Weiyu Wang http://orcid.org/0000-0002-3768-4886

References

[1] Bray F, Ferlay J, Soerjomataram I, et al. Global cancer statistics 2018: GLOBOCAN estimates of incidence and mortality worldwide for 36 cancers in 185 countries. CA Cancer J Clin. 2018;68(6):394–424.

[2] Ferlay J, Colombet M, Soerjomataram I, et al. Estimating the global cancer incidence and mortality in 2018: GLOBOCAN sources and methods. Int J Cancer. 2019;144(8):1941–1953.

[3] Marcos-Gragera R, Mallone S, Kiemeney LA, et al., EUROCARE-5 Working Group. Urinary tract cancer survival in Europe 1999-2007: results of the population-based study EUROCARE-5. Eur J Cancer. 2015;51(15):2217–2230.

[4] Yan H, Xie H, Ying Y, et al. Pioglitazone use in patients with diabetes and risk of bladder cancer: a systematic review and meta-analysis. Cancer Manag Res. 2018;10:1627–1638.

[5] Freedman ND, Silverman DT, Hollenbeck AR, et al. Association between smoking and risk of bladder cancer among men and women. JAMA. 2011;306(7):737–745.

[6] Richters A, Aben K, Kiemeney L. The global burden of urinary bladder cancer: an update. World J Urol. 2019;38(8):1895–1904. Advance online publication.

[7] McConkey DJ, Choi W, Ochoa A, et al. Intrinsic subtypes and bladder cancer metastasis. Asian J Urol. 2016;3(4):260–267.

[8] Bartel DP. MicroRNAs: target recognition and regulatory functions. Cell. 2009;136(2):215–233.

[9] Wang X, Liang Z, Xu X, et al. miR-148a-3p represses proliferation and EMT by establishing regulatory circuits between ERBB3/AKT2/c-myc and DNMT1 in bladder cancer. Cell Death Dis. 2016;7(12):e2503.
[10] Xie L, Li S, Lin Y, et al. MicroRNA-124-3p inhibits cell migration and invasion in bladder cancer cells by targeting ROCK1. J Transl Med. 2013;11(1):276.
[11] Li J, Xu X, Meng S, et al. MET/SMAD3/SNAIL circuit mediated by miR-323a-3p is involved in regulating epithelial-mesenchymal transition progression in bladder cancer. Cell Death Dis. 2017;8(8):e3010.
[12] Yan H, Li J, Ying Y, et al. MIR-300 in the imprinted DLK1-DIO3 domain suppresses the migration of bladder cancer by regulating the SP1/MMP9 pathway. Cell Cycle. 2018;17(24):2790–2801.
[13] Xu X, Zhu Y, Liang Z, et al. c-Met and CREB1 are involved in miR-433-mediated inhibition of the epithelial-mesenchymal transition in bladder cancer by regulating Akt/GSK-3β/Snail signaling. Cell Death Dis. 2016;7(2):e2088.
[14] Xu X, Chen H, Lin Y, et al. MicroRNA-409-3p inhibits migration and invasion of bladder cancer cells via targeting c-Met. Mol Cells. 2013;36(1):62–68.
[15] Hu Z, Lin Y, Chen H, et al. MicroRNA-101 suppresses motility of bladder cancer cells by targeting c-Met. Biochem Biophys Res Commun. 2013;435(1):82–87.
[16] Li S, Xu X, Xu X, et al. MicroRNA-490-5p inhibits proliferation of bladder cancer by targeting c-Fos. Biochem Biophys Res Commun. 2013;441(4):976–981.
[17] Lin Y, Chen H, Hu Z, et al. miR-26a inhibits proliferation and motility in bladder cancer by targeting HMGA1. FEBS Lett. 2013;587(15):2467–2473.
[18] Benetatos L, Hatzimichael E, Londin E, et al. The microRNAs within the DLK1-DIO3 genomic region: involvement in disease pathogenesis. Cell Mol Life Sci. 2013;70(5):795–814.
[19] Lehner B, Kunz P, Saehr H, et al. Epigenetic silencing of genes and microRNAs within the imprinted Dlk1-Dio3 region at human chromosome 14.32 in giant cell tumor of bone. BMC Cancer. 2014;14(1):495.
[20] Haga CL, Phinney DG. MicroRNAs in the imprinted DLK1-DIO3 region repress the epithelial-to-mesenchymal transition by targeting the TWIST1 protein signaling network. J Biol Chem. 2012;287(51):42695–42707.
[21] Thiery JP, Acloque H, Huang RY, et al. Epithelial-mesenchymal transitions in development and disease. Cell. 2009;139(5):871–890.
[22] Yilmaz M, Christofori G. EMT, the cytoskeleton, and cancer cell invasion. Cancer Metastasis Rev. 2009;28(1–2):15–33.
[23] Wu Y, Zhou BP. Snail: more than EMT. Cell Adh Migr. 2010;4(2):199–203.
[24] Hoot KE, Lighthall J, Han G, et al. Keratinocyte-specific Smad2 ablation results in increased epithelial-mesenchymal transition during skin cancer formation and progression. J Clin Invest. 2008;118(8):2722–2732.
[25] Lamouille S, Xu J, Derynck R. Molecular mechanisms of epithelial-mesenchymal transition. Nat Rev Mol Cell Biol. 2014;15(3):178–196.
[26] Zhou B, Guo W, Sun C, et al. Linc00462 promotes pancreatic cancer invasiveness through the miR-665/TGFBR1-TGFBR2/SMAD2/3 pathway. Cell Death Dis. 2018;9(6):706.
[27] Zhang M, Wang S, Yi A, et al. microRNA-665 is down-regulated in gastric cancer and inhibits proliferation, invasion, and EMT by targeting PPP2R2A. Cell Biochem Funct. 2020;38(4):409–418. Advance online publication.
[28] Wang S, Du S, Lv Y, et al. MicroRNA-665 inhibits the oncogenicity of retinoblastoma by directly targeting high-mobility group box 1 and inactivating the Wnt/β-catenin pathway. Cancer Manag Res. 2019;11:3111–3123.
[29] Kulis M, Esteller M. DNA methylation and cancer. Adv Genet. 2010;70:27–56.
[30] Hay ED. An overview of epithelio-mesenchymal transformation. Acta Anat. 1995;154(1):8–20.
[31] Tse JC, Kalluri R. Mechanisms of metastasis: epithelial-to-mesenchymal transition and contribution of tumor microenvironment. J Cell Biochem. 2007;101(4):816–829.
[32] Xu J, Lamouille S, Derynck R. TGF-beta-induced epithelial to mesenchymal transition. Cell Res. 2009;19(2):156–172.
[33] Hao Y, Baker D, Ten Dijke P. TGF-β-Mediated Epithelial-Mesenchymal Transition and Cancer Metastasis. Int J Mol Sci. 2019;20(11):2767.
[34] Wu S, Chen J, Dong P, et al. Global gene expression profiling identifies ALDH2, CCNE1 and SMAD3 as potential prognostic markers in upper tract urothelial carcinoma. BMC Cancer. 2014;14(1):836.
[35] Massagué J, Seoane J, Wotton D. Smad transcription factors. Genes Dev. 2005;19(23):2783–2810.
[36] Guaita S, Puig I, Franci C, et al. Snail induction of epithelial to mesenchymal transition in tumor cells is accompanied by MUC1 repression and ZEB1 expression. J Biol Chem. 2002;277(42):39209–39216.
[37] Miyoshi A, Kitajima Y, Sumi K, et al. Snail and SIP1 increase cancer invasion by upregulating MMP family in hepatocellular carcinoma cells. Br J Cancer. 2004;90(6):1265–1273.
[38] Herranz N, Pasini D, Díaz VM, et al. Polycomb complex 2 is required for E-cadherin repression by the Snail1 transcription factor. Mol Cell Biol. 2008;28(15):4772–4781.
[39] Vincent T, Neve EP, Johnson JR, et al. A SNAIL1-SMAD3/4 transcriptional repressor complex promotes TGF-beta mediated epithelial-mesenchymal transition. Nat Cell Biol. 2009;11(8):943–950.
[40] Ikenouchi J, Matsuda M, Furuse M, et al. Regulation of tight junctions during the epithelium-mesenchyme transition: direct repression of the gene expression of claudins/occludin by Snail. J Cell Sci. 2003;116(10):1959–1967.